COMPDYN 2011
ECCOMAS Thematic Conference on
Computational Methods in Structural Dynamics and Earthquake Engineering
M. Papadrakakis, M. Fragiadakis, V. Plevris (eds.)
Corfu, Greece, 25-28 May 2011

DAMAGE ASSESSMENT OF HYPERBOLIC PARABOLOIDAL SHELLS USING FINITE ELEMENT UPDATING

Rafael Castro[1], **Demosthenes Talaslidis**[2], **Rafael Gallego**[3] **and Guillermo Rus**[3]

[1]University of Cordoba
Department of Mechanics, Campus de Rabanales, 14071 Cordoba, Spain
e-mail: me1catrr@uco.es

[2] Aristotle University Thessaloniki
Department of Civil Engineering, Mail Stop 502, 54124 Thessaloniki, Greece
e-mail: talaslid@civil.auth.gr

[3] University of Granada
Department of Structural Mechanics, Campus de Fuentenueva, 18071 Granada, Spain
e-mail: {gallego,grus}@ugr.es

Keywords: Finite Element Updating, Structural Damage, Structural Dynamics, Hyperbolic Paraboloidal Shells.

Abstract. *Assessment of the structural and functional integrity of civil engineering structures is an essential design issue and of continuous concern during the process of maintenance, repair and upgrading of such structures. The concept of Structural Health Monitoring (SHM) offers means to predict the structural behavior of a particular structure under operating conditions that differ from those taken into consideration in the initial design cycle. Employment of the aforementioned concept requires computational models that are verified, refined and adjusted with respect to actual measurements. In this paper, a finite element updating methodology is presented, which aims to reduce the discrepancies between the dynamic model parameters of the structure and the measurements. A sucessful finite element updating approach must rely on physically meaningful criteria for selecting the updating parameters and the most suitable method in order to modify the mass and stiffness matrices of the computational model. The proposed iterative method is based on a generalized variational principle, a modified version of the Hu-Washizu principle of elastodynamics, which treats displacements, rotations, strains and stresses as independent variables that can be treated as updating parameters. Thus, a more efficient and direct implementation of measurements is possible. Furthermore, the discretization yields simple and effective finite elements especially suited to repetitious computations required in dynamic finite element updating. Different parameter sensitivities are studied. Single and multi-objective optimization processes are carried out using objective functions that include the eigenfrequencies and the strain modal energy of the structure. Finally, some alternative damage scenarios are presented in order to validate the proposed formulation for the case of hyperbolic paraboloidal shell structures.*

1 INTRODUCTION

Assessment of the structural and functional integrity of civil engineering structures is an essential design issue and of continuous concern during the process of maintenance, repair and upgrading of such structures. The concept of Structural Predictive Maintenance (SPM) offers means to predict the structural behavior of a particular structure under operating conditions that differ from those taken into consideration in the initial design cycle. Employment of the aforementioned concept requires computational models that are verified, refined and adjusted with respect to actual measurements. The finite element updating method is employed to minimize those differences. Over the past decades, significant research has been performed in this area [1]. The monograph by Friswell [2] and the review article [3] mainly deal with the different steps in the updating procedure. Furthermore, Brownjohn *et al.* [4] focus on those steps by using a controlled laboratory-based study of a simple structure. Finite element modelling for updating is the first phase. In case of an updating process, the development of a finite element model for a civil engineering structure, differs from the finite element models used for common structural analysis purposes. Some important issues must be taken into consideration [5]: type of elements, boundary conditions and the presence of damage. Civil engineering structures are modelled by beam, plate, shell, and solid elements with thousands of degrees of freedom (displacements and rotations). An important issue is that not all degrees of freedom can be measured; also rotations are difficult to assess. Therefore, it is vital to employ finite elements that restrict the number of rotational degrees of freedom to a minimum. Furthermore, the element formulation should contain physically meaningful updating parameters. Selection of the appropriate updating parameters is crucial to the finite element updating process. A small perturbation of some parameters may affect the behavior of the structure, while other parameters not. The former may not necessarily be the ideal candidates for an updating process. Therefore, it is necessary to develop a sensitivity analysis preceded by an error localisation investigation. If some damage is present, the model has to take it also into account in order to realistically model the structure. The Force Balance Method [6] calculates a residual force vector, that if plotted can represent the non-equilibrated forces/moments in direction of the degrees of freedom; a fact that points to an error in the modelling phase. Sensitivity analysis represents the variation of an objective function with respect to structural parameters [7, 8]. The derivation of the objective functions can be performed by four different methodologies [9]: overall finite differences, discrete derivatives, continuum derivatives, and computational or automatic differentitation. The selection of a proper objective function can ensure an efficient sensitivity analysis [10]. The objective function establishes a relationship between the measurement results and the numerical predictions. Modal properties such as eigenfrequencies and mode shapes of a structure are normally employed in these objective functions. An optimization process serves to minimize the differences between experimental and numerical results [11–14]. Finally, to ensure the agreement of the updating results it is necessary to validate them. Towards this aim, some validation techniques are employed (e.g., Modal Assurance Criterion [15]).

In this paper, a finite element updating methodology is presented, which aims to reduce the discrepancies between the dynamic model parameters of the structure and the measurements. An effective finite element updating approach must rely on physically meaningful criteria for selecting the updating parameters and the most suitable method in order to modify the mass and stiffness matrices of the computational model. The proposed iterative method employs finite elements that are derived using a generalized variational principle, a version of the Hu-Washizu principle of elastodynamics. This variational principle treats displacements, rotations, strains, and stresses as independent variables that can be selected in a direct manner as updating parameters. The changes of these parameters are estimated by employing both single- and multi-objective optimisation processes. The application of the method is illustrated by employing four-noded doubly-curved shell elements with a total number of twenty degrees of freedom to study different cases such as damaged or undamaged models. Numerical examples demonstrate that the proposed approach is stable and produces accurate results.

2 FINITE ELEMENT MODELLING

2.1 Hyperbolic Paraboloidal shell

The accuracy of the method is demonstrated for the case of a homogeneous, isotropic, and thin hyperbolic paraboloidal shell (hypar shell) of rectangular planform with length a, width b, thickness h, and radii of curvature R_x and R_y, (see figure 1). The dimensions of the hypar shell are:

$$a = 20\,m \quad b = 20\,m \quad R_y = \frac{b}{0.1} \quad R_x = -R_y \quad h = 0.2\,m \tag{1}$$

Young's modulus and Poisson's ratio are taken as $2 \cdot 10^{10}\ N/mm^2$ and 0.3, respectively.

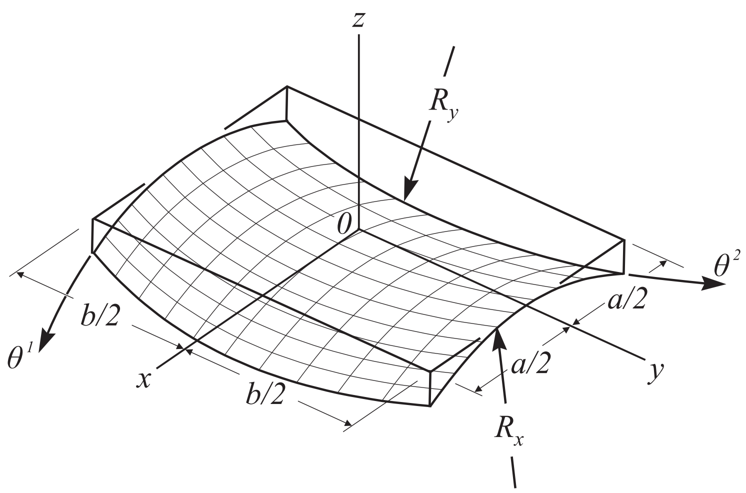

Figure 1: Hyperbolic paraboloidal shell with rectangular planform.

A damage scenario is considered with a stiffness reduction in two parts of the hypar (see figure 2). A uniform mesh with 8×8 elements is used. Eigenfrequencies and mode shapes obtained from computational methods for the damaged model of this hypar shell are condisered to be the experimental results to be validated.

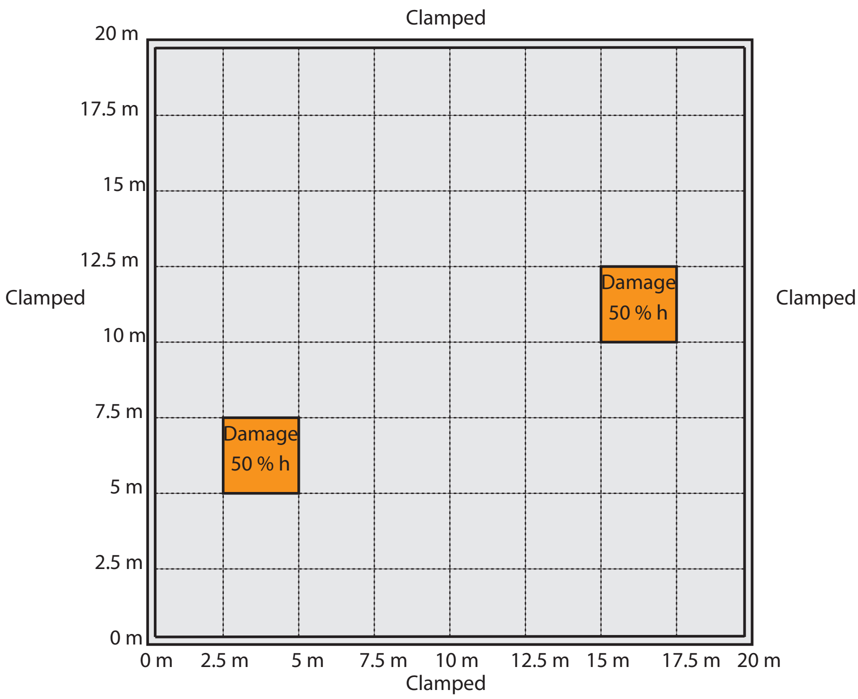

Figure 2: Damage scenario for the hyperbolic paraboloidal shell.

2.2 Finite element formulation

The shell element derived in the present study is a four-noded, doubly-curved isoparametric finite element with five degrees of freedom at each node: three physical components of the displacements u_1, u_2, u_3 and two components of the rotations φ_1, φ_2. Bilinear shape functions N_k are chosen for the physical components of the displacements and rotations:

$$\begin{aligned} & u_i = \sum_{k=1}^{4} u_i^k \, N_k \qquad \varphi_\alpha = \sum_{k=1}^{4} \varphi_\alpha^k \, N_k \\ \text{with} \quad & N_k = \frac{1}{4} \left(1 + \xi_k \, \xi\right) \left(1 + \eta_k \, \eta\right) \quad i = 1, 2, 3 \quad \alpha = 1, 2 \end{aligned} \tag{2}$$

Denoting by $\mathcal{U}(\boldsymbol{\gamma})$ the strain energy and by $\boldsymbol{\gamma}$ and $\boldsymbol{\sigma}$ the vectors containing the strain and stress components, respectively, a version of the generalized Hu-Washizu principle assumes the form [16]:

$$\Pi_{HW} \left[\mathbf{v}, \boldsymbol{\gamma}, \boldsymbol{\sigma}\right] = \int_V \left[\mathcal{U}(\boldsymbol{\gamma}) - \boldsymbol{\sigma}^T \left(\boldsymbol{\gamma} - \mathbf{D}\,\mathbf{v}\right) - \Pi_b\right] dV - \int_{S_{\hat{v}}} \left(\mathbf{v} - \hat{\mathbf{v}}\right) \boldsymbol{\sigma}\,\mathbf{n}\, dS - \int_{S_t} \Pi_t \, dS \tag{3}$$

In the variational principle (3), $\mathbf{v}$ represents the displacement vector and the index b refers to the body forces. The vector $\hat{\mathbf{v}}$ denotes prescribed displacements on the part of the boundary, where displacements are prescribed $(S_{\hat{v}})$. If the body forces in V and surface tractions on S_t are conservative, then Π_b and Π_t denote the corresponding potentials.

As mentioned before, the use of the Hu-Washizu principle and the independent approximation of strain and stress yields a series of desirable features important for the reliability, convergence behavior, and efficiency of the elemental formulation, e.g., avoidance of superfluous energy and zero energy modes. Furthermore, the discrete approximation is drawn in a consistent manner from the general theory of the continuum and the mechanical behavior of the finite element, without resource to special manipulations or computational procedures. Also, it has been shown (see [16, 17]) that essential prerequisites for the achievement of these goals are: The identification of the constant and higher-order deformational modes that are contained in the displacement/rotation assumptions, the realization that constant terms are neccesary for convergence and that higher-order terms reappear in different strain components. Therefore, our approximations need not retain the higher-order terms in two different strain components (they are needed only to inhibit a mode). Suppressing such terms serves to reduce excessive internal energy and to improve convergence. As an example, the following assumptions for the extensional strains have been shown to serve the aforementioned goals:

$$\begin{aligned} \varepsilon_{11} &= \bar{\varepsilon}_{11} + \bar{\bar{\varepsilon}}_{11}\,\eta \\ \varepsilon_{22} &= \bar{\varepsilon}_{22} + \bar{\bar{\varepsilon}}_{22}\,\xi \\ \varepsilon_{12} &= \bar{\varepsilon}_{12} + \underline{\bar{\bar{\varepsilon}}_{11}\,\xi} + \underline{\bar{\bar{\varepsilon}}_{22}\,\eta} \end{aligned} \tag{4}$$

The higher order modes $(\bar{\bar{\varepsilon}}_{11}, \bar{\bar{\varepsilon}}_{22})$ in the expression for the shear strain ε_{12} appear also in the expressions for the strains ε_{11} and ε_{22}. In order to avoid succesive energy, the assumption for the shear strain should not contain the underlined terms.

The eigenvalue problem for the undamped free vibration problem takes the well-known form:

$$\mathbf{K}\,\mathbf{u_i} = \omega_i^2\,\mathbf{M}\,\mathbf{u_i} \tag{5}$$

where $\mathbf{K}$ is the stiffness matrix of the system, ω_i is the natural frequency in radians of mode i, $\mathbf{u_i}$ represent the corresponding eigenvector, and $\mathbf{M}$ is the mass matrix of the structure. The consistent element mass matrix is derived by discretizing the kinetic energy:

$$\delta\mathcal{U}_K = \frac{1}{2}\int_V \rho\, 2\,\mathbf{v}\,\delta\ddot{\mathbf{v}} dV \tag{6}$$

$$\tag{7}$$

In table 1, numerical results are presented for the nondimensional frequency parameter λ given by:

$$\lambda = \omega\, a\, b\sqrt{\frac{\rho\, h}{D}} \qquad D = \frac{E\, h^3}{12\,(1-\nu^2)} \tag{8}$$

that demonstrate the convergence behavior for different meshes.

Damage identification based on changes in vibration characteristics requires that those changes are reliable. In table 2, the variation of λ for various ratios b/h is presented. These results are illustrated graphically by figure 3. From these results it can be concluded that the frequency vibration characteristic could not be used alone in a damage identification process due to its relatively low variation with thickness changes.

Mode	Mesh 6×6	Mesh 8×8	Mesh 10×10	Mesh 12×12
1	52.76	51.817	51.39	51.17
2	94.41	86.72	83.69	82.16
3	94.41	86.72	83.69	82.16
4	132.73	121.84	117.41	115.13
5	215.96	170.22	155.32	148.33
6	216.86	170.92	155.94	148.91
7	243.54	200.88	186.51	179.64
8	243.54	200.88	186.51	179.64
9	326.76	269.19	249.10	239.35
10	579.75	329.97	275.19	252.20

Table 1: Convergence behavior of frequency parameter ($\lambda = \omega ab\sqrt{\rho h/D}$) for the clamped (CCCC) thin hyperbolic paraboloidal shell of figure 1.

Mode	$b/h = 200$	175	150	125	100	75	50	25	10
1	80.77	73.02	65.53	58.40	51.81	46.01	41.28	37.72	33.78
2	100.91	96.74	92.96	89.61	86.72	84.31	82.22	78.99	67.37
3	100.91	96.74	92.96	89.61	86.72	84.31	82.22	78.99	67.37
4	129.04	126.90	124.99	123.31	121.84	120.48	118.85	114.00	93.63
5	179.26	176.61	174.24	172.13	170.22	168.31	165.61	156.38	120.29
6	179.64	177.08	174.79	172.76	170.92	169.08	166.44	157.32	121.51

Table 2: Variation of frequency parameter ($\lambda = \omega ab\sqrt{\rho h/D}$) with respect to thickness for the clamped (CCCC) thin hyperbolic paraboloidal shell of figure 1.

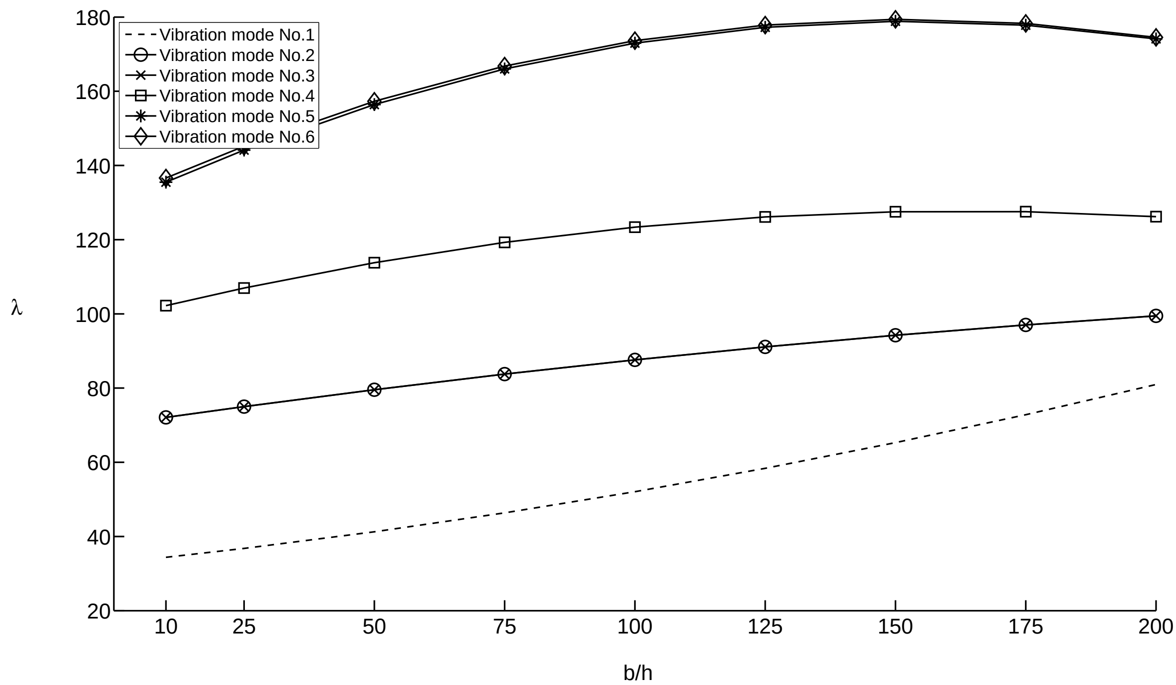

Figure 3: Graphical representation of the variation of frequency parameter ($\lambda = \omega ab\sqrt{\rho h/D}$) with respect to the thickness

3 CORRELATION

Analytical results from a finite element model must be validated with respect to those obtained by experimental measurements. Towards this aim, several techniques may be employed [19]. One of the simplest methods for data correlation is to calculate the percentage differences between the natural frequencies obtained by analytical and experimental techniques (see fourth column of table 3 and figure 4).

Mode	Undamaged hypar (Hz)	Damaged hypar (Hz)	Differences (%)	MAC (%)
1	3.60	3.59	0.28	0.99
2	6.02	5.98	0.73	0.008
3	6.02	6.02	-0.01	0.008
4	8.47	8.38	1.01	0.99
5	11.83	11.54	2.45	0.64
6	11.88	11.78	0.78	0.64
7	13.96	13.69	1.91	0.11
8	13.96	13.80	1.17	0.11
9	18.71	18.45	1.38	0.97
10	22.93	22.06	3.83	0.71

Table 3: Differences in the first ten natural frequencies between the undamaged and damaged model for the CCCC hypar (8×8 mesh) of figure 1.

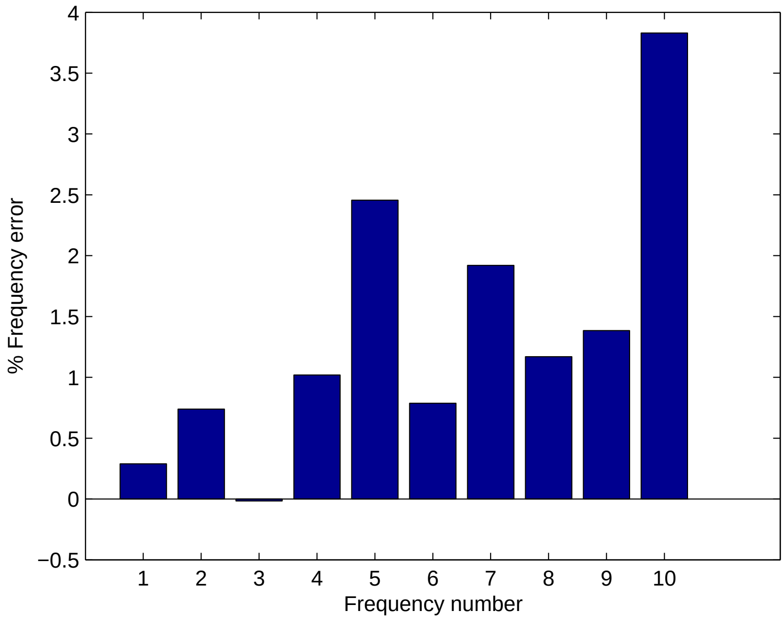

Figure 4: Percentage differences between analytically and experimentally obtained natural frequencies.

The modal assurance criterion (MAC) is another commonly used method to establish a correlation factor for each pair of analytical and experimental mode shapes:

$$MAC_{ij} = \frac{\left|\boldsymbol{\phi}_{a_i}^T \boldsymbol{\phi}_{e_j}\right|^2}{\left(\boldsymbol{\phi}_{a_i}^T \boldsymbol{\phi}_{a_i}^T\right)\left(\boldsymbol{\phi}_{e_j}^T \boldsymbol{\phi}_{e_j}^T\right)} \tag{9}$$

A high correlation yields a MAC value close to 1, whereas a low correlation assumes values near 0. The fifth colum of table 3 presents MAC values for the undamaged model of the hypar (analysis using doubly-curved shell elements) and those for the damaged hypar scenario (considered as experimental data). Furthermore, figure 5 represents the MAC-matrix for the first ten mode shapes.

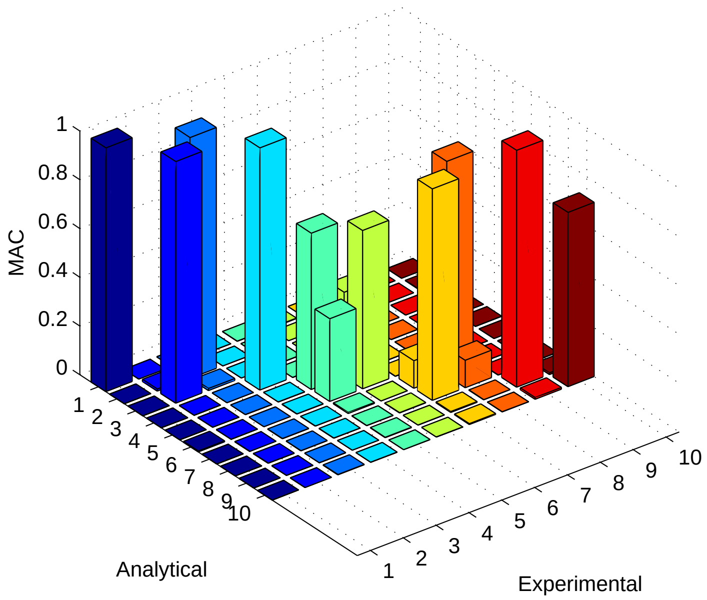

Figure 5: Representation of Modal Assurance Criterion (MAC) matrix between the undamaged and damaged models for the CCCC hypar.

4 OBJECTIVE FUNCTIONS AND SENSITIVITY ANALYSIS

Jaishi [11] proposed the use of two objective functions comprised of the discrepancies between experimental and numerical results. The modal strain energy residual function (Π_1) and the eigenfrequency residual function (Π_2) are defined as:

$$\Pi_1(p) = \frac{1}{\Pi_1(p_0)} \sum_{i=1}^{m} \left(\frac{\boldsymbol{\phi}_{ai}^T \mathbf{K} \boldsymbol{\phi}_{ai}}{\boldsymbol{\phi}_{ei}^T \mathbf{K} \boldsymbol{\phi}_{ei}} - 1 \right)^2 \qquad \Pi_2(p) = \frac{1}{\Pi_2(p_0)} \sum_{i=1}^{m} \left(\frac{\lambda_{ai}}{\lambda_{ei}} - 1 \right)^2 \tag{10}$$

where λ and $\boldsymbol{\phi}$ denote the m eigenfrequencies and modal vectors of the eigenvalue problem, the subindices ai and ei refer to the analytical and experimental results that in this case correspond to the undamaged and damaged models. Matrix $\mathbf{K}$ represents the stiffness matrix of the system and the variable p is defined as a normalization of model parameters (i.e., the thickness h of the bridge) between the initial (h_0) and updated values (h):

$$p_h = -\frac{h - h_0}{h_0} \qquad h = h_0(1 - p_h) \tag{11}$$

Sensitivity analysis of these objective functions with respect to the model parameters is carried out by forming the gradients of the objective functions Π_1 and Π_2, respectively (derivatives of Π_1 and Π_2 with respect to the parameter p_j):

$$\frac{\partial \Pi_1}{\partial p_j} = \frac{1}{\Pi_1(p_0)} \sum_{i=1}^{m} \left[2 \frac{A}{(\boldsymbol{\phi}_{ei}^T \mathbf{K} \boldsymbol{\phi}_{ei})^2} \left(\frac{\boldsymbol{\phi}_{ai}^T \mathbf{K} \boldsymbol{\phi}_{ai}}{\boldsymbol{\phi}_{ei}^T \mathbf{K} \boldsymbol{\phi}_{ei}} - 1 \right) \right] \tag{12}$$

$$A = \left[\left\{ \left(\boldsymbol{\phi}_{ei}^T \mathbf{K} \boldsymbol{\phi}_{ei} \right) \left[2 \frac{\partial \boldsymbol{\phi}_{ai}^T}{\partial p_j} \mathbf{K} \boldsymbol{\phi}_{ai} + \boldsymbol{\phi}_{ai}^T \frac{\partial \mathbf{K}}{\partial p_j} \boldsymbol{\phi}_{ai} \right] \right\} - \left\{ \left(\boldsymbol{\phi}_{ai}^T \mathbf{K} \boldsymbol{\phi}_{ai} \right) \left(\boldsymbol{\phi}_{ai}^T \frac{\partial \mathbf{K}}{\partial p_j} \boldsymbol{\phi}_{ai} \right) \right\} \right] \tag{13}$$

$$\frac{\partial \Pi_2}{\partial p_j} = \frac{1}{\Pi_2(p_0)} \sum_{i=1}^{m} \left[2 \left(\frac{\lambda_{ai}}{\lambda_{ei}^2} - \frac{1}{\lambda_{ei}} \right) \frac{\partial \lambda_{ai}}{\partial p_j} \right] \tag{14}$$

For the derivatives:

$$\frac{\partial \lambda_i}{\partial p_j} \qquad \frac{\partial \boldsymbol{\phi}_i}{\partial p_j} \tag{15}$$

in equations (13) and (14), the expressions derived by Fox and Kapoor [18] are employed:

$$\frac{\partial \lambda_i}{\partial p_j} = \boldsymbol{\phi}_i^T \left[\frac{\partial \mathbf{K}}{\partial p_j} - \lambda_i \frac{\partial \mathbf{M}}{\partial p_j} \right] \boldsymbol{\phi}_i \tag{16}$$

$$\frac{\partial \boldsymbol{\phi}_i}{\partial p_j} = \sum_{q=1}^{d} \beta_{jiq} \boldsymbol{\phi}_q \qquad \beta_{jiq} = \begin{cases} \boldsymbol{\phi}_q^T \left[\left(\frac{\partial \mathbf{K}}{\partial p_i} - \lambda_j \frac{\partial \mathbf{M}}{\partial p_i} \right) / (\lambda_j - \lambda_q) \right] \boldsymbol{\phi}_j & q \neq j \\ -\frac{1}{2} \boldsymbol{\phi}_j^T \frac{\partial \mathbf{M}}{\partial p_i} \boldsymbol{\phi}_j & q = j \end{cases} \tag{17}$$

where d denotes the number of modes that will be considered in the evaluation. Since in a hypar model only few of the modes can be computed and the lower modes are of importance, it is reasonable to consider here only the first ten modes ($m = d = 10$). Furthermore, the derivatives of the stiffness and mass matrix, appearing in equations (16) and (17) are formed rather analytically than numerically using finite differences. This yields a series of advantages in the optimization process.

Figure 6(a) and figure 6(b) illustrate the sensitivity of the objective functions Π_1 and Π_2 with respect to variations of the thickness parameter. It can be observed that the strain modal energy function easily detects both damages. On the other hand, sensitivity of the objective function Π_2, which is related to the eigenfrequencies, assumes a symmetrical form that can not identify the position of the damages. Nevertheless, eigenfrequencies can be accurately measured by operational modal analysis and therefore are considered useful in the optimization process.

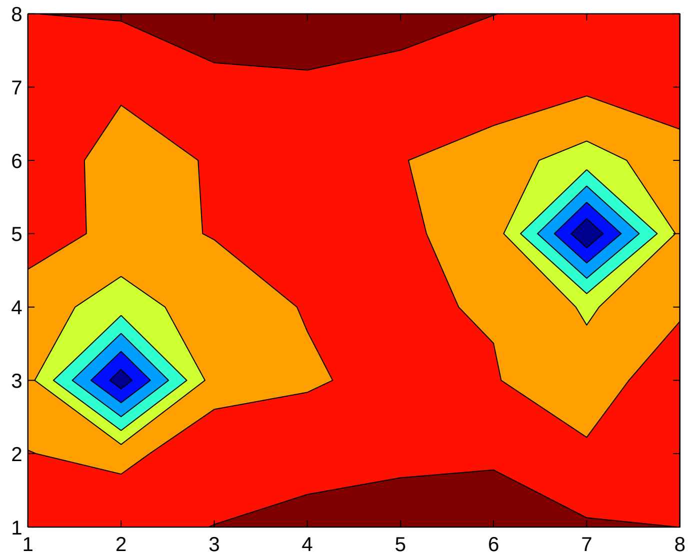

(a) Sensitivity of the objective function Π_1 with respect to thickness.

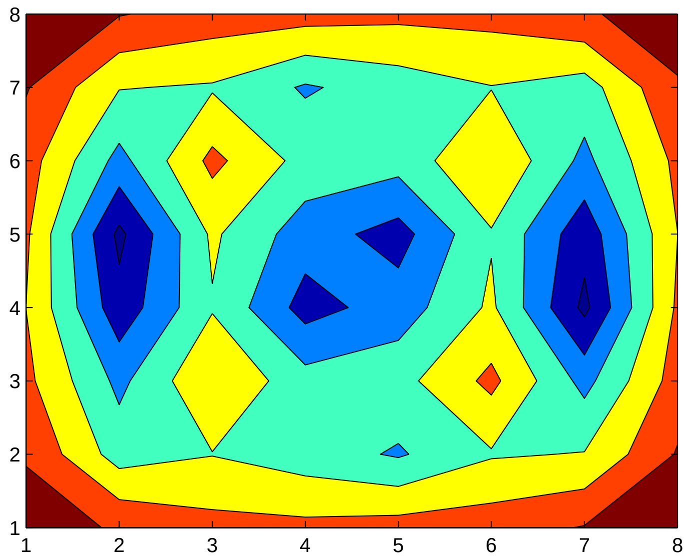

(b) Sensitivity of the objective function Π_2 with respect to thickness.

Figure 6: Sensitivity analysis of objective functions with respect to thickness.

5 SELECTION OF UPDATING PARAMETERS

As mentioned before, selection of the updating parameters is the most difficult step in an updating process and the accuracy of the results strongly depends upon this election. Finite element models with fine mesh configurations may lead to thousands of degrees of freedom. Furthermore, considering material properties of individual elements may lead to a very large number of updated parameters related to Young's modules, thickness, etc. Also, selection of updating parameters would be more difficult, if some damage scenario is considered. For these reasons, an error localisation approach and substructuring techniques are needed.

5.1 Error localisation

In view of possible damage scenarios, the optimization process would become more effective if a method is established for updating parameters that considers this particular case. The Force Balance Method (FBM) calculates a residual vector [6, 19]:

$$\mathbf{F}_r = (\mathbf{K}_a - \lambda_{e_r}\mathbf{M}_a)\,\boldsymbol{\phi}_{e_r} \tag{18}$$

that represents for each mode r the inaccuracies of the finite element model by plotting the degrees of freedom that are not in equilibrium. For illustrative purposes, non-balanced forces (moments) corresponding to the degrees of freedom of the finite element model for the damaged bridge are represented in figure 7.

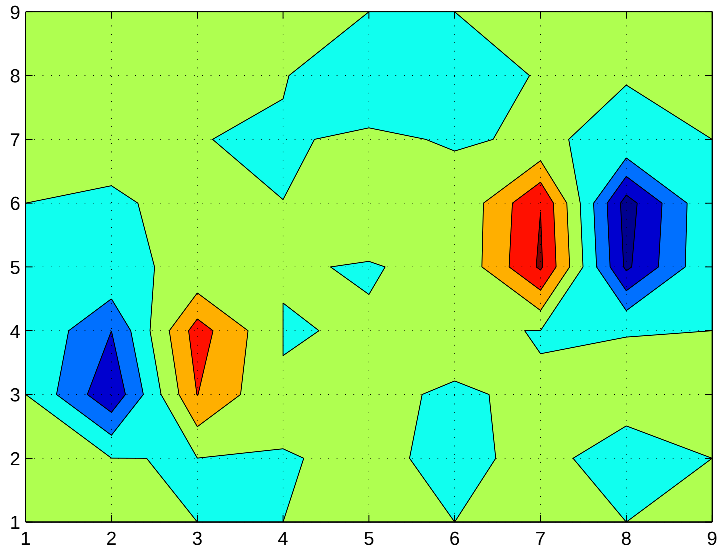

Figure 7: Error localisation based on Force Balance Method plotted for the first mode.

5.2 Substructure method for parameter selection

Model updating is a process that could lead to ill-conditioned problems, if the same number of updating parameters with respect to each finite element of the model is selected. A common and physically meaningful approach, the so-called "substructure method," is to establish updating parameters for different groups of finite elements. Kim and Park [20, 21] proposed an automated parameter selection procedure for multi-objective optimisation problems. This method relies on the fact that two neighboring parameters p_i and p_j can be merged into one updating parameter, if the sensitivity with respect to the objective functions has the same sign. This yields a map in the structure with different areas associated with identical parameters.

In the present work, a new method to implement substructure divisions of the finite element model has been developed. By assuming that high sensitivities are associated with damaged zones, a priorization selection procedure is established. The sensitivity vector, that stores in each row the sensitivity of each element with respect to the objective function is classified by zones. These zones correspond to multiples of the semi-difference sensitivity extreme (maximum and minimum) absolut values, called step. To illustrate the method, figure 8 shows a substructure division for ten zones.

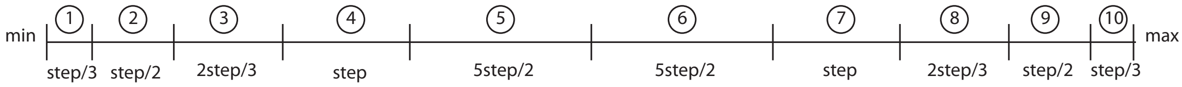

Figure 8: Substructure method.

In the case of the current hypar shell, the relationship between the element thickness and the updating parameters assumes the form:

$$\mathbf{H} = \mathbf{H_0} - h_0 \mathbf{S_b} \mathbf{P_h} \tag{19}$$

where $\mathbf{H}$ is a column vector that contains the hypar element thicknesses, vector $\mathbf{H_0}$ stores the reference thickness taken as h_0. Matrix $\mathbf{S_b}$, called *substructure-matrix*, is defined by the method explained before and assumes the following form:

$$\mathbf{S_b} = \begin{bmatrix} 1 & 0 & \dots & 0 & 0 \\ 1 & 0 & \dots & 0 & 0 \\ 0 & 0 & \dots & 0 & 1 \\ 0 & 1 & \dots & 0 & 0 \\ \vdots & \vdots & \vdots & \vdots & \vdots \\ 1 & 0 & 0 & \dots & 0 \end{bmatrix} \tag{20}$$

with the number of rows equal to the number of finite elements in the model and with the total number of columns equal to the number of non-dimensional updating variables, p_{h_i}. According to the matrix (20), every row consists of zeros except for a single element equal to one.

6 COMPUTATIONAL PROCEDURE

The computational work, related to the present finite element updating methodology, has been developed by programing several subroutines using MATLAB. Furthermore, “fmincon” and “fgoalattain” gradient-based MATLAB optimization algorithms are employed for single-objective and multi-objective optimization, respectively.

7 NUMERICAL EXAMPLES

In order to demonstrate the applicability of the proposed method, some numerical results are presented for the case of the damaged hypar of figure 2. Two different updating processes are studied, the first one considers a single-objective optimization by using a linear combination of objective functions $\Pi_1(p)$ and $\Pi_2(p)$ defined as follows:

$$\Pi_3(p) = \frac{1}{\Pi_1(p_0)} \sum_{i=1}^{m} \left(\frac{\boldsymbol{\phi}_{ai}^T \mathbf{K} \boldsymbol{\phi}_{ai}}{\boldsymbol{\phi}_{ei}^T \mathbf{K} \boldsymbol{\phi}_{ei}} - 1 \right)^2 + \frac{1}{\Pi_2(p_0)} \sum_{i=1}^{m} \left(\frac{\lambda_{ai}}{\lambda_{ei}} - 1 \right)^2 \tag{21}$$

and the second one considers a multi-objective optimisation process using the same objective functions but separately.

The convergence plots (figure 9(a) and figure 9(b)) show that for both, single-objective and multi-objective optimization, convergence is achieved in a similar way after ten iterations. The multi-objective optimization process shows that the results fluctuate in the first iterations due to the particular optimization process of the objective functions Π_1 and Π_2 to find a Pareto optimal. Furthermore, the objective function Π_2 is more difficult to optimize. The reason for such complication is the low sensitivity with respect to damage, as it was shown in figure 6(b).

Figures 10(a)-10(b) and tables 4-5 demonstrate that the proposed method is capable to localize all damaged elements. Additionally, correlation of modal shapes is high since the MAC factor is nearly 1.

Mode	Undamaged hypar (Hz)	Damaged hypar (Hz)	After updating (Hz)	Differences (%)	MAC (%)
1	3.6	3.59	3.59	0.15	100
2	6.02	5.98	5.98	0.14	100
3	6.02	6.02	6.02	-0.63	99.99
4	8.47	8.38	8.38	-0.30	99.99
5	11.83	11.54	11.54	-0.57	99.89
6	11.88	11.78	11.78	-0.003	99.98
7	13.96	13.69	13.69	-0.41	99.74
8	13.96	13.80	13.80	-0.15	99.68
9	18.71	18.45	18.45	-0.33	99.92
10	22.93	22.06	22.06	-0.16	99.67

Table 4: Frequency differences and MAC between the damaged and updated model for single-objective optimization of function Π_3

Mode	Undamaged hypar (Hz)	Damaged hypar (Hz)	After updating (Hz)	Differences (%)	MAC (%)
1	3.60	3.59	3.59	0.15	100
2	6.02	5.98	5.98	0.14	99.99
3	6.02	6.02	6.02	-0.63	99.98
4	8.47	8.38	8.38	-0.30	99.98
5	11.83	11.54	11.54	-0.59	99.89
6	11.88	11.78	11.79	-0.006	99.98
7	13.96	13.69	13.69	-0.41	99.88
8	13.96	13.80	13.80	-0.16	99.85
9	18.71	18.45	18.46	-0.34	99.92
10	22.93	22.06	22.08	-0.18	99.64

Table 5: Frequency differences and MAC between the damaged and updated model for multi-objective optimization of functions Π_1 and Π_2

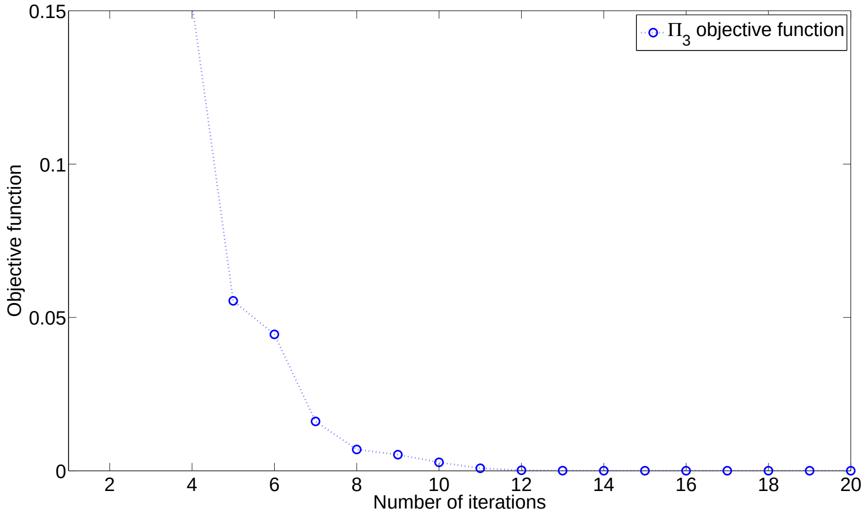

(a) Convergence behavior of the single-optimization process for objective function Π_3.

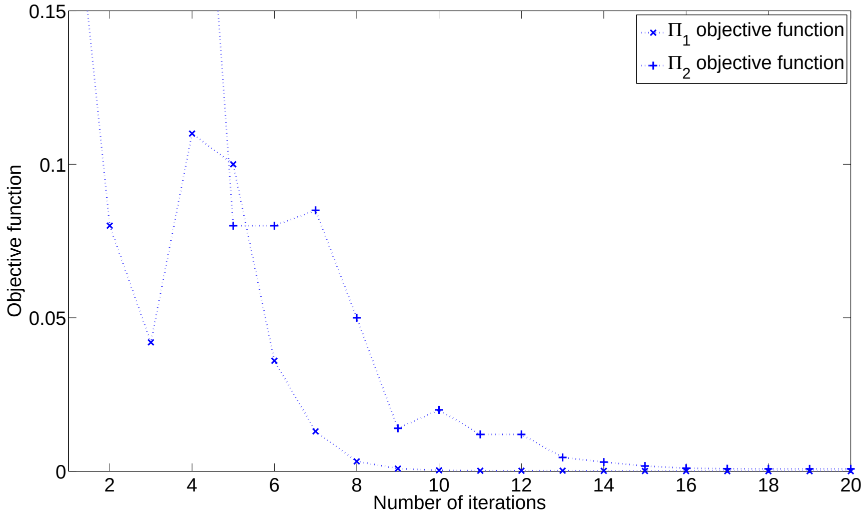

(b) Convergence behavior of the multi-objective optimization process for objective function Π_1 and Π_2.

Figure 9: Optimization convergence behavior.

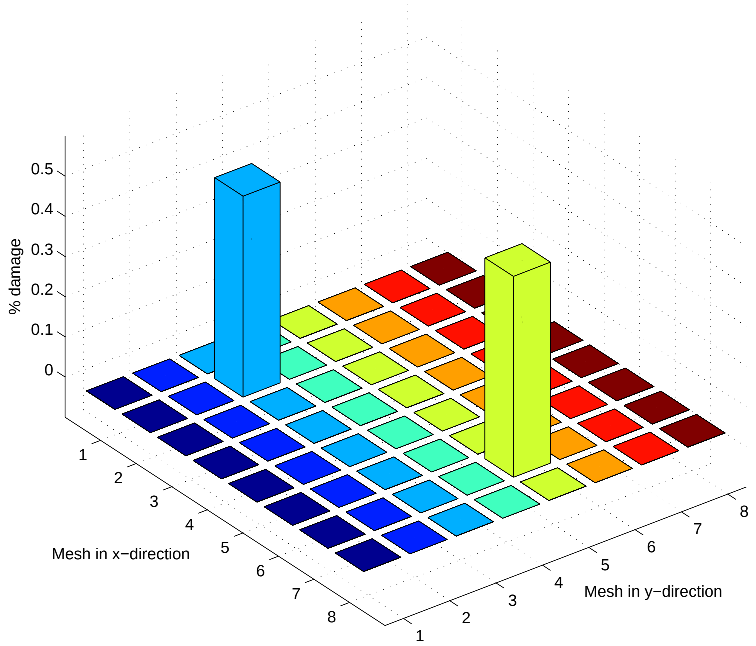

(a) Damage localization and severity after updating by single-objective optimization of function Π_3.

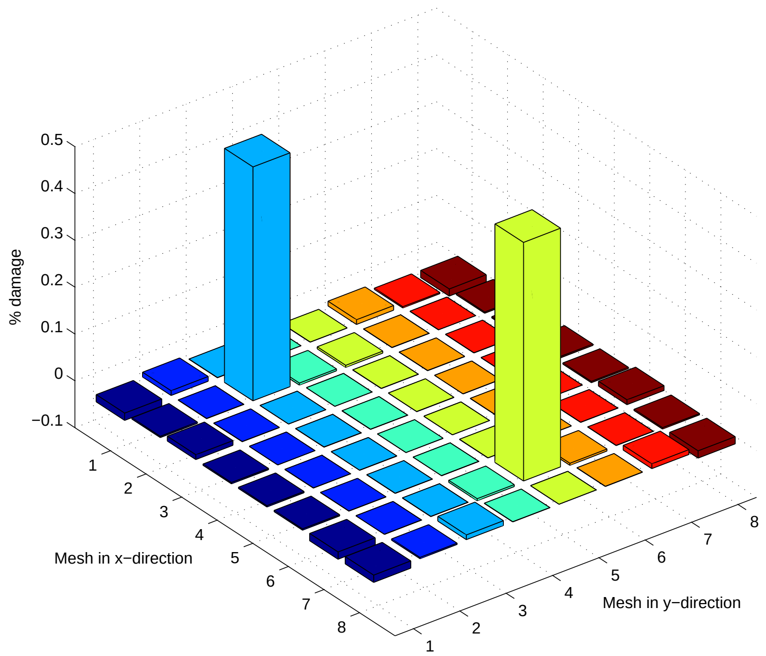

(b) Damage localization and severity after updating by multi-objective optimization of function Π_1 and Π_2.

Figure 10: Damage localization and severity.

7.1 Noisy vibration measurements

Vibration measurements are often contaminated by noise. It could be originated by the wind, the traffic, and also due to the cables that are connected to the accelerometers. This uncertainty can be simulated by adding some noisy-terms to the experimental modal shapes [22]:

$$\boldsymbol{\phi}_{e_j}^{noisy} = \boldsymbol{\phi}_{e_j} + \boldsymbol{\alpha}_j \, RMS(\boldsymbol{\phi}_{e_j}) \, \psi \tag{22}$$

where $\boldsymbol{\alpha}_j$ is a random matrix generated by a Gaussian distribution of mean 0 and standard deviation 1, ψ is an scalar that represents the noise level and RMS is the root mean square given by:

$$RMS(\boldsymbol{\phi}_{e_j}) = \sqrt{\frac{1}{N_j} \sum_{j=1}^{N_j} (\boldsymbol{\phi}_{e_j})^2} \tag{23}$$

For illustrative purposes, this methodology is followed for the case of the damaged hypar of figure 2 with a noise level of $0.5\,\%$. In this case, only single-objective optimization is employed (objective function Π_3). The optimization convergence is illustrated in figure 11. Table 6 shows the differences before and after updating the model . Frequency differences are plotted in figure 12. The damage localization, see figure 13, illustrates differences in the percentage of damage severity due to the effect of the noise.

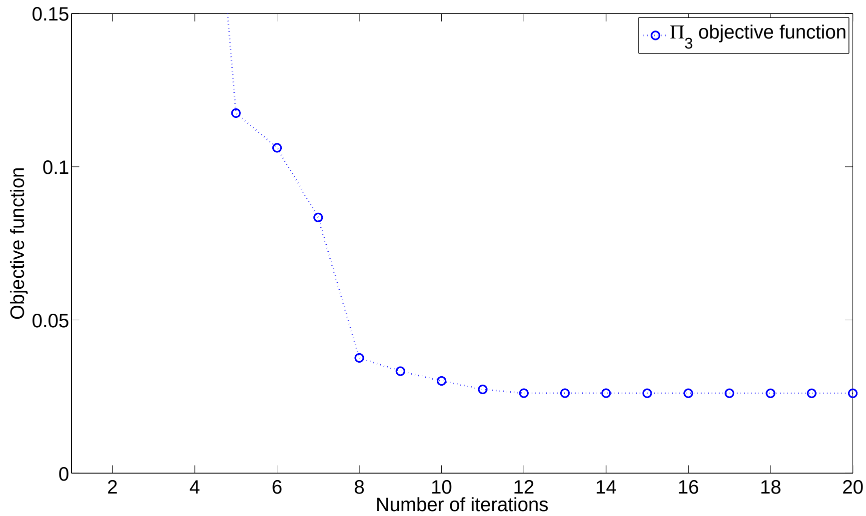

Figure 11: Convergence behavior of the single-optimization process for objective function Π_3 with noisy data.

Mode	Undamaged hypar (Hz)	Damaged hypar (Hz)	After updating (Hz)	Differences (%)	MAC (%)
1	3.60	3.59	3.59	0.14	100
2	6.02	5.98	5.97	-0.02	88.98
3	6.02	6.02	6.02	-0.44	89.02
4	8.47	8.38	8.40	-0.28	99.96
5	11.83	11.54	11.53	-0.64	99.85
6	11.88	11.78	11.77	-0.02	99.93
7	13.96	13.69	13.68	-0.34	99.88
8	13.96	13.80	13.79	-0.20	99.87
9	18.71	18.45	18.44	-0.43	99.91
10	22.93	22.06	22.05	-0.24	99.24

Table 6: Frequency differences and MAC between the damaged and updated model for single-objective optimization of function Π_3 with noisy data.

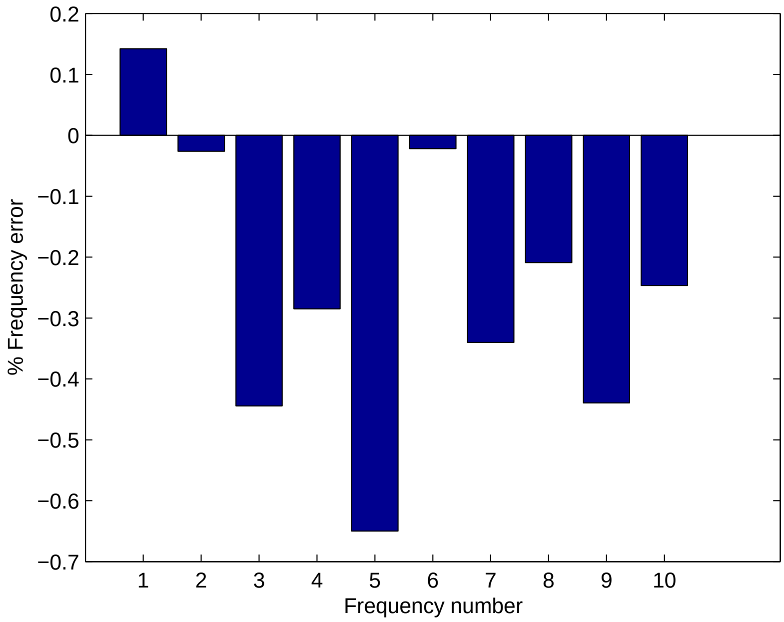

Figure 12: Percentage differences between analytical and noisy natural frequencies.

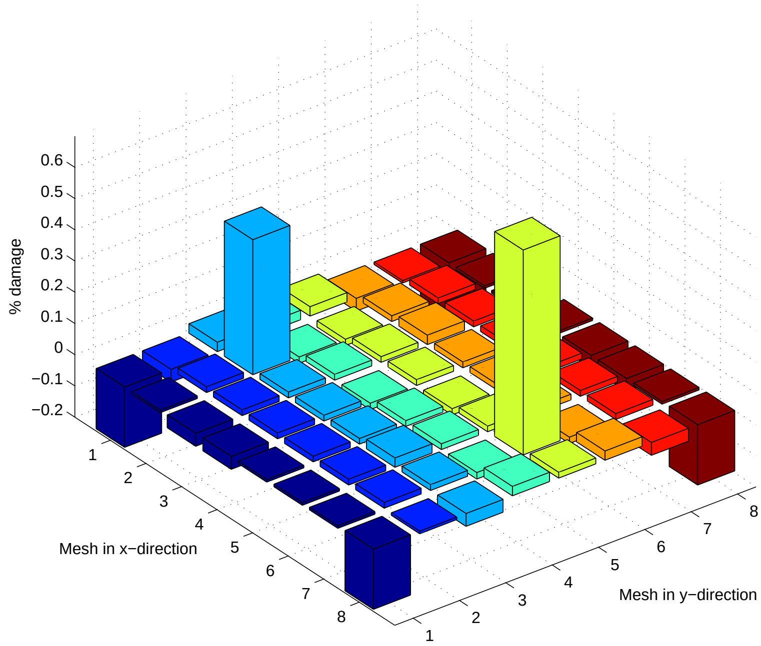

Figure 13: Damage localization and severity after updating the single-objective optimization of function Π_3 with noisy data.

8 CONCLUSIONS

In this paper, a finite element updating methodology is presented. Finite element modelling is carried out by using doubly-curved shell elements based on the variational principal of Hu-Washizu. The formulation possesses some important features that ensure low computational effort and reliable results. A hypar model with different damages is employed to test the accuracy of the proposed methodology. Eigenfrequencies and mode shapes of the damaged model are considered as experimental data that are used in the updating process of the numerical model. In order to study the confidence between the numerical and experimental results, several correlation techniques are employed.

The present methodology makes use of sensitivity for updating parameter selection. Two different objective functions are employed to determine the sensitivity of the model: modal strain energy residual and eigenfrequencies residual. High sensitivity zones are associated with possible damaged elements and are classified by the use of a simple-priorization technique. In order to establish the correspondence between the element parameters in the numerical model and the updating parameters, some matrix operations have been developed.

The performance of the method is demonstrated by presenting case studies for single-objective and multi-objective optimization. In the first case study, a linear combination of modal strain energy and eigenfrequencies residual functions was selected as objective function. On the contrary, in the case of multi-objective optimization process, both objective functions were independently employed. The results with respect to localization and severity of the damage are in good agreement with the damaged model. Furthermore, the convergence of the optimization process is achieved in both cases after a few iterations, thus revealing that the proposed approach produces an efficient and accurate computational tool suitable for complicated structural systems.

REFERENCES

[1] P. Avitabile, Model updating - Endless possibilities, *Sound and Vibration*, 2000.

[2] M.I. Friswell, J.E. Mottershead, *Finite element model updating in structural dynamics*, Kluwer Academic Publishers, 1995.

[3] J.E. Mottershead, M.I. Friswell, Model updating in structural dynamics: A survey, *Journal of Sound and Vibration*, **167**, 347–375, 1993.

[4] J.M.W. Brownjohn, Pin-Qi Xia, Hong Hao, Yong Xia, Civil structure condition assessment by FE model updating: Methodology and case studies, *Finite Elements in Analysis and Design*, **37**, 761–775, 2001.

[5] H.G. Natke, Problems of model updating procedures: A perspective resumption, *Mechanical Systems and Signal Processing*, **12**, 65–74, 1998.

[6] E. Fissette, S. Ibrahim, C. Stavrinidis, Error location and updating of analytical dynamic models using a force balance method, *Proceedings of the 6th International Modal Analysis Conference*, Kissimmee, Florida, 1998.

[7] L. Gil Espert, *Análisis de sensibilidad con comportamiento no lineal del material y su aplicación en el diseño asistido de estructuras*. PhD Thesis, Universidad Politécnica de Cataluña, Spain ,1997.

[8] S. Hernández, Del diseño convencional al diseño óptimo. Posibilidades y variantes. Part I: Análisis de sensibilidad y optimización local y global, *Revista Internacional de Métodos Numéricos para Cálculo y Diseño en Ingeniería*, **9**, 91–110, 1993.

[9] F. van Keulen, R.T. Haftka, N.H. Kim, Review of options for structural design sensitivity analysis. Part 1: Linear systems, *Computer Methods in Applied Mechanics and Engineering*, **194**, 3213–3243, 2005.

[10] Bijaya Jaishi, Wei-Xin Ren Structural finite element model updating using ambient vibration test results, *Journal of Structural Engineering*, **131**, 617–628, 2005.

[11] Bijaya Jaishi, Wei-Xin Ren, Finite element model updating based on eigenvalue and strain energy residuals using multiobjective optimisation technique, *Mechanical Systems and Signal Processing*, **21**, 2295–2317, 2007.

[12] R.T. Haftka, Z. Gurdal, *Elements of Structural Optimization*, Kluwer Academic Publishers, 1992.

[13] Kyung K. Choi, Nam-Ho Kim, *Structural Sensitivity Analysis and Optimization 1. Linear Systems*. Springer, 2005.

[14] S. Hernández, Del diseño convencional al diseño óptimo. Posibilidades y variantes. Part II: Optimización multiobjectivo y sensibilidad de la solución óptima, *Revista Internacional de Métodos Numéricos para Cálculo y Diseño en Ingeniería*, **9**, 259–270, 1993.

[15] R.J. Allemang, The modal assurance criterion-Twenty years of use and abuse, *Sound and Vibration*, 2003.

[16] G. Wempner, D. Talaslidis, *Mechanics of Solids and Shells*. CRC Press, 2003.

[17] G. Wempner, D. Talaslidis, C. Hwang, A simple and efficient approximation of shells via quadrilateral elements, *Journal of Applied Mechanics*, **49**, 115–120, 1982.

[18] R.L. Fox, M.P. Kapoor, Rates of change of eigenvalues and eigenvectors, *AIAA Journal*, **6**, 2426–2429, 1968.

[19] W. Heylen, S. Lammens, P. Sas, *Modal Analysis Theory and Testing*. Katholieke Universiteit Leuven, Departement Werktuigkunde, Leuven, 1997.

[20] Gyenong-Ho Kim, Youn-Sik Park, An improved updating parameter selection method and finite element model update using multiobjective optimisation technique, *Mechanical Systems and Signal Processing*, **18**, 59–78, 2004.

[21] Gyenong-Ho Kim, Youn-Sik Park, An improved updating parameter selection method and finite element model update using multiobjective optimisation technique, *Journal of Sound and Vibration*, **309**, 778–793, 2008.

[22] R. Palma, G. Rus, R. Gallego, Probabilistic inverse problem and system uncertainties for damage detection in piezoelectrics. *Mechanics of Materials*, **41**, 1000–1016, 2009.